Metabolic Exchange

DOI: 10.1002/anie.201101225

Connecting Chemotypes and Phenotypes of Cultured Marine Microbial Assemblages by Imaging Mass Spectrometry**

*Yu-Liang Yang, Yuquan Xu, Roland D. Kersten, Wei-Ting Liu, Michael J. Meehan, Bradley S. Moore, Nuno Bandeira, and Pieter C. Dorrestein**

Since the early days of bacterial culturing over a century ago, microbiologists have known that microorganisms respond to their surroundings. Unicellular organisms rely on metabolic exchange to adapt to environmental stresses, sense colony density, occupy niches within hosts, and form biofilms.[1–7] For example, *Bacillus subtilis* utilizes metabolic exchange to lyse neighboring microbes, including siblings, during sporulation,[8–10] whereas other forms of metabolic exchange, such as the secretion of siderophores, stimulate the growth and development of *Streptomyces* and uncultured bacteria.[11,12] Despite the importance of chemistry in biology, studies that connect chemotypes and phenotypes to adaptive microbial behavior in Petri dishes, including signaling and chemical warfare, have largely relied on indirect measurements for individual chemotypes and phenotypes. To connect the chemotypes and phenotypes in this study, we used MALDI-based imaging mass spectrometry (IMS)[13–16] to observe the chemical output and metabolic exchange of a marine microbial assemblage in two dimensions.

The ability to monitor the two-dimensional distribution of a wide array of metabolites simultaneously from a complex mixture of distinct organisms opens the door to comprehensive analyses of interspecies signaling interactions within a microbial assemblage in a spatial fashion. Analysis of the spatial distribution of these metabolites enables the generation of a testable hypothesis with respect to functions of the observed chemotypes, without the immediate need to know the structural characteristics. IMS provides the ability to correlate the presence of metabolites to phenotypic changes and to detect new chemotypes and/or phenotypes that cannot be observed by the naked eye. In this way, IMS enables prioritization of the molecules to be targeted for identification through proteomic and metabolomic approaches or to be subjected to mass spectrometry guided isolation and nuclear magnetic resonance based structure elucidation. Understanding of these molecular networks and interactions will illuminate how microbes respond to neighboring organisms and in turn influence and alter the growth of their neighbors.

We demonstrate that IMS can be used to observe the chemical output within complex microbial assemblages. This information can then be used to prioritize the organisms and molecules for structural characterization. It is important to prioritize the molecules because the structural characterization of the molecules is one of the rate-limiting steps in our understanding of chemical cross-talk between organisms. We collected the marine microbial assemblage by scraping the slimy surface of a barnacle located on the pier of the Scripps Institution of Oceanography (University of California, San Diego), which extends into the Pacific Ocean. IMS was used to visualize the interactions between members of the microbial assemblage obtained from this barnacle and grown on solid media. Because a typical soil sample contains 10^8 colony-forming units (CFUs) per gram of soil, and an ocean sample typically contains 10^5 CFUs per milliliter of water, we anticipated that we would observe large numbers of colonies from this environmental sample. Therefore, the barnacle scrapings were serially diluted onto agar plates. Subsequently, the heterogeneous mixture of microorganisms was allowed to grow at 28 °C for 3 days (Figure 1 a). Once distinct colonies were visible, a 4 cm by 2 cm region of agar was cut, laid on top of a MALDI target plate, and covered with a matrix of α-cyano-4-hydroxycinnamic acid and 2,5-dihydroxybenzoic acid. The matrix is required for the ionization of the molecules present along the surface of the sample. At the same time, the matrix effectively fixes the organisms in place when applied.

Once covered with a matrix coating, the sample was subjected to IMS. IMS enables the visualization of metabolites that are secreted into the growth medium, as well as metabolites associated with the colonies themselves. Nine signals and their distributions are highlighted in Figure 1 c. Each ion distribution is superimposed over the section of Figure 1 a enclosed in the rectangle. Five of the signals are associated with colonies, and four are due to metabolites

[*] W.-T. Liu, Prof. Dr. P. C. Dorrestein
Department of Chemistry and Biochemistry
University of California, San Diego
Biomedical Science Building (BSB), Room 4090
9500 Gilman Drive, MC 0636, La Jolla, CA 92093-0636 (USA)
E-mail: pdorrest@ucsd.edu
Dr. Y.-L. Yang,[+] Dr. Y. Xu,[+] M. J. Meehan, Prof. Dr. B. S. Moore, Prof. Dr. N. Bandeira, Prof. Dr. P. C. Dorrestein
Skaggs School of Pharmacy and Pharmaceutical Sciences
University of California, San Diego, CA (USA)
R. D. Kersten, Prof. Dr. B. S. Moore, Prof. Dr. P. C. Dorrestein
Center for Marine Biotechnology and Biomedicine
Scripps Institution of Oceanography
University of California, San Diego, CA (USA)
Prof. Dr. N. Bandeira
Department of Computer Science and Engineering
University of California, San Diego, CA (USA)
[+] These authors contributed equally.

[**] Funding was provided by the Beckman Foundation and NIH grants GM085770 (B.S.M), 1-P41-RR024851 (N.B.), and NIH GM08283 and AI095125 (P.C.D.). W.-T.L. was supported, in part, by a study-aboard grant (SAS-98116-2-US-108) from Taiwan. We thank Elizabeth Shank for critically reviewing the manuscript.
Supporting information for this article is available on the WWW under http://dx.doi.org/10.1002/anie.201101225.

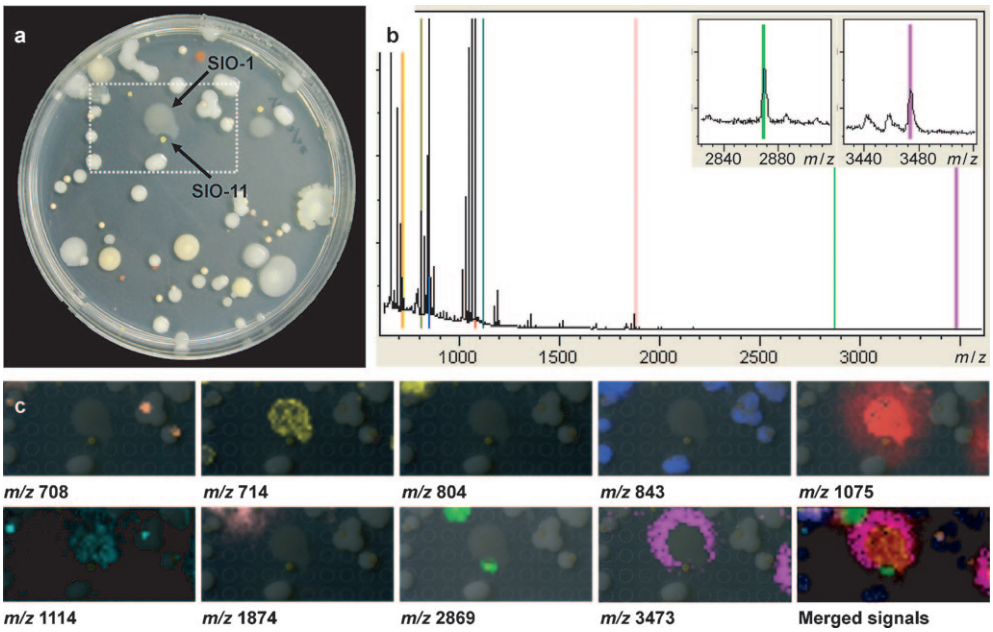

Figure 1. Source and visualization of the chemical output of the marine microbial assemblage. a) Photograph of the microorganisms isolated from the slimy layer of the barnacles and grown on yeast extract–malt extract (ISP-2) in a Petri dish (diameter 100 mm, height 1.5 mm). b) Average mass spectrum of a total of 1681 spectra collected during the IMS experiment. The ions that were visualized with different colors are highlighted. c) Spatial distribution of the signals. The mass corresponding to the ions is provided below the images. In these images, the most abundant ions are shown with a 1 Da window.

secreted into the agar medium. On the basis of the imaging data alone, two organisms from the marine sample that each influenced the physiology of the other were investigated more closely.

The IMS data suggested that one secreted metabolite with a mass of 2869 Da from organism SIO-11 (Scripps Institution of Oceanography-organism 11) inhibited the motility of organism SIO-1. The interactions observed between these two organisms were confirmed when SIO-11 and SIO-1 were grown in isolation from the rest of the microbial assemblage: SIO-11 inhibited the motility of a monoculture SIO-1 through the secretion of a metabolite (*m*/*z* 2869), and at the same time, the presence of SIO-1 resulted in the production of additional metabolites (*m*/*z* 727, 729, 743, 765, 781, and 796) in SIO-11 in a time-dependent manner at the juncture where the two organisms physically interacted (Figure 2a). When SIO-11 was grown by itself for 120 h, only the molecules with a mass of 2869 Da were observed (see Figure 20 in the Supporting Information). This example illustrates the multifaceted nature of microorganism interactions and that IMS provides testable hypotheses. In this way, IMS enabled prioritization of the organisms and molecules associated with the signals at both *m*/*z* 2869 and 743 for further structural and functional characterization.

We then sought to identify the signals observed by IMS (Figure 1). In this endeavor, the species information based on 16S rDNA sequencing was directly informative, as our research group had previously characterized the metabolic output of *B. subtilis*, which was identical in 16S rDNA to SIO-1 (see Figure 5 in the Supporting Information).[15] Indeed, the mass-spectral profile of SIO-1 was remarkably similar to that of *B. subtilis* 3610, and the ions at *m*/*z* 714 (partially characterized polyglutamate), 1075 (surfactin), 1545 (plipastatin), and 3475 (subtilosin) were observed for both strains, as confirmed by TOF/TOF analysis (see Figures 6–8 in the Supporting Information).[15] There were also several metabolites that were associated with other colonies. Tandem MS analysis identified one metabolite (*m*/*z* 843) to be related to the polyglutamate (*m*/*z* 714), but with an additional glutamate moiety (see Figure 9 in the Supporting Information). On the basis of their distribution, these polyglutamates may be components of the extracellular matrix or cell-wall material. Among the most interesting signals observed by IMS, however, was that at *m*/*z* 2869 due to an unknown molecule secreted by SIO-11, because this signal overlaps with the region in which SIO-1 did not grow, and six additional mass spectrometry signals due to unknown molecules at *m*/*z* 727, 729, 743, 765, 781, and 796, which were observed when SIO-11 was cultured adjacent to SIO-1.

To obtain the unknown metabolites for further structural and functional characterization, we extracted cultures of SIO-11 grown for 72 h in A1 medium at 28 °C with MeOH and acetone and then purified the extracts by mass spectrometry guided isolation involving size-exclusion and reversed-phase chromatography. The purified peptide responsible for the signal at *m*/*z* 2869 (peptide 2869) inhibited the motility of *B. subtilis* SIO-1 when a quantity as little as 0.035 nmol was spotted onto an agar plate (Figure 2b). High-resolution mass spectrometry (Fourier transform ion cyclotron resonance (FTICR) MS) indicated that the observed neutral monoisotopic mass was 2866.65 Da (see Figure 10 in the Supporting Information). Because the genome for SIO-11 is not available, peptide 2869 was subjected to multiple stages of tandem mass spectrometry and was determined to be a peptide through the combined use of Spectral Networks (see Figure 12 in the Supporting Information), a proteomics algorithm that enables the alignment and de novo sequencing of multistage tandem mass spectrometry data.[17,18] The sequence was determined by de novo sequencing and NMR spectroscopic interpretation to be MSVVDIVSTLLDSLGITIAQLRVLIGL with an *N*-formyl group at methionine (see Figures 11–19 and Tables 1 and 2 in the Supporting Information). Because peptide 2869 did not suppress the growth of SIO-1, the results imply that the function of this peptide,

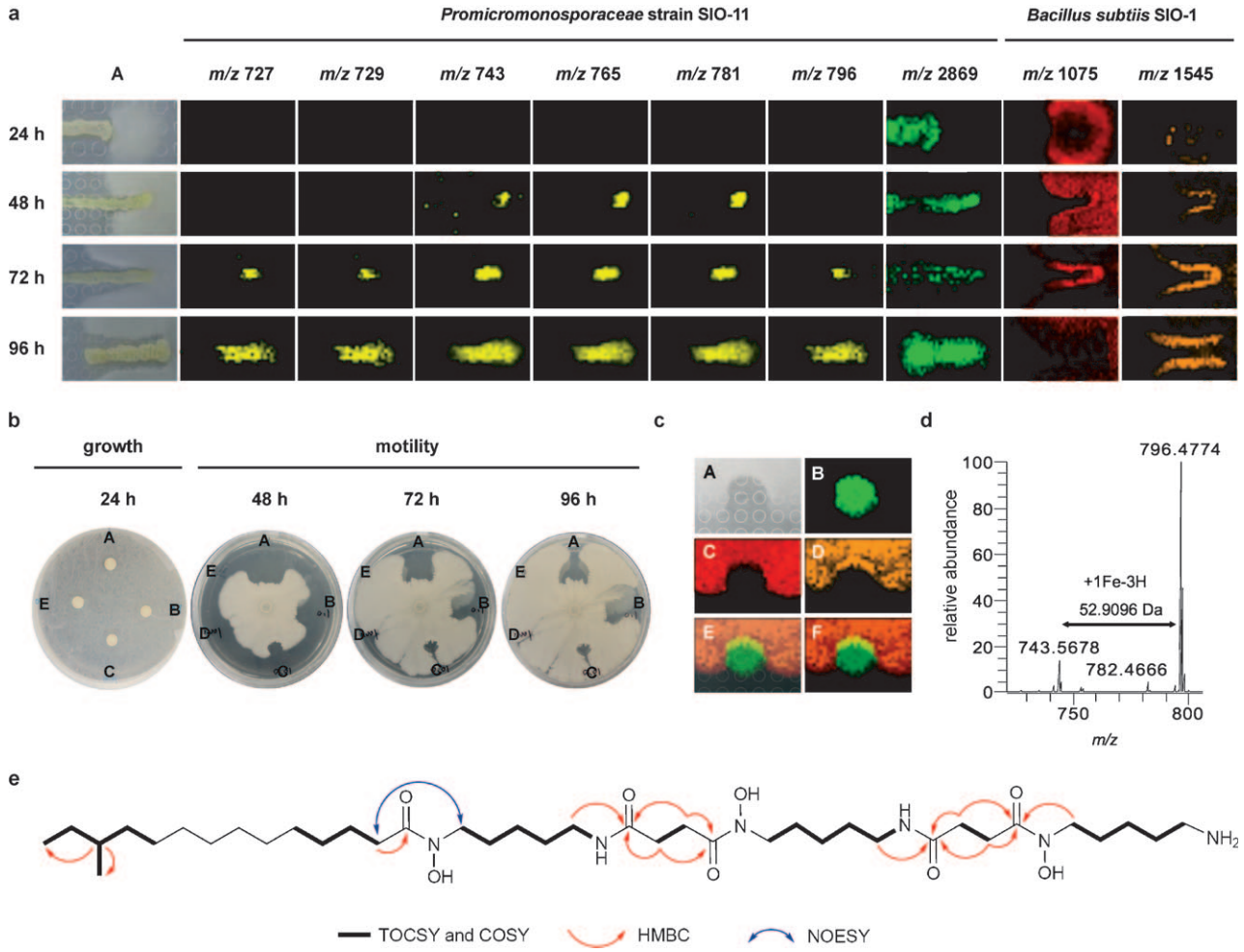

Figure 2. Interaction between *Bacillus subtilis* SIO-1 and *Promicromonosporaceae* strain SIO-11. a) Time-course IMS of SIO-1 and SIO-11 cocultures. The siderophores (*m*/*z* 727 $[M+H]^+$, 729 $[M+H]^+$, 743 $[M+H]^+$, 765 $[M+Na]^+$, 781 $[M+K]^+$, 796 $[M+Fe-2H]^+$) and peptide 2869 (*m*/*z* 2869 $[M+H]^+$) were produced by SIO-11. Surfactin (*m*/*z* 1075 $[M+K]^+$) and plipastatin (*m*/*z* 1545 $[M+K]^+$) were produced by SIO-1. Promicroferrioxamine (*m*/*z* 743 $[M+H]^+$, 765 $[M+Na]^+$, and 781 $[M+K]^+$) was observed after coculture for 48 h, and the signal for the iron-chelating compound (*m*/*z* 796 $[M+Fe-2H]^+$) was observed after 72 h. Two additional siderophores (*m*/*z* 727 $[M+H]^+$ and 729 $[M+H]^+$) were detected after coculture for 72 h. These ions were not observed when SIO-11 was cultured alone on the agar medium (see Figure 20 in the Supporting Information). In these images, the IMS signals are shown with a 1 Da window. Column A shows photographs of the colonies. b) Functional evaluation of peptide 2869 from SIO-11. The growth of SIO-1 was not affected by peptide 2869 in the first 24 h. The motility of SIO-1 was halted when SIO-1 reached the spot treated with A) 10 μg, B) 1 μg, or C) 0.1 μg of peptide 2869; D) treatment with 0.01 μg of peptide 2869; E) blank control. c) IMS of SIO-1 treated with purified peptide 2869: A) photograph of the SIO-1 colonies; B) IMS picture of signal *m*/*z* 2869 $[M+H]^+$; C) IMS picture of signal *m*/*z* 1075 $[M+K]^+$; D) IMS picture of signal *m*/*z* 1545 $[M+K]^+$; E) superimposed image of (A–D); F) superimposed image of (B–D). d) Two ions observed by FTICR MS, at *m*/*z* 743.5678 $[M+H]^+$ and *m*/*z* 796.4774 $[M+Fe-2H]^+$, provided the first indication that this molecule was a siderophore. e) Structure of promicroferrioxamine with correlations observed by 2D NMR spectroscopy.

produced by the nonmotile SIO-11, is to prevent mobile bacteria, such as a motile *B. subtilis* strain, from entering its growth niche (see Figure 4 in the Supporting Information). From an ecological standpoint, the inhibition of motility is a creative approach for a nonmotile bacterium to protect itself and to establish a colony among other motile bacteria (Figure 2b,c).

Because several metabolites produced by SIO-11 were only upregulated in the presence of SIO-1, they were quite difficult to isolate in large enough quantities for structural elucidation. Therefore, we prepared 600 100 mm agar plates containing cocultured SIO-1 and SIO-11. Subsequently, the cells at the interface of the two organisms were harvested and extracted. Following gel filtration and HPLC purification, compounds with masses of 743 and 796 Da (Figure 2d) were isolated. The mass differences between the observed IMS signal at *m*/*z* 743 and those at *m*/*z* 765 and 781 were due to a sodium ion and a potassium ion, which were removed during purification. It was not clear why there was an observed mass at *m*/*z* 796 until the sample was analyzed by high-resolution mass spectrometry. High-resolution mass spectrometry (FTICR MS) showed two major signals: one at *m*/*z* 743.5678 $[M+H]^+$ and another at *m*/*z* 796.4774. These masses correspond to the molecular formulas $C_{38}H_{74}N_6O_8$ and $C_{38}H_{71}N_6O_8Fe$ and provided the first indication that this compound was an iron chelator, also known as a side-

rophore.[8] Furthermore, the peak at *m*/*z* 796.4774 displayed the characteristic iron isotopic profile (see Figure 27 in the Supporting Information). We named this compound promicroferrioxamine because of the functional and structural similarity to commercially utilized desferrioxamine and 16S rDNA phylogenetic analysis of the producing organism (see Figure 5 in the Supporting Information).[11] Microorganisms of marine origin often produce siderophores that are key components for the establishment of microbial communities.[12,19] The compounds with masses of *m*/*z* 727 and 729 are structurally related to promicroferrioxamine; thus, SIO-11 secreted an array of siderophores in response to the presence of SIO-1 (see Figures 29–32 in the Supporting Information).

To determine the structure of promicroferrioxamine, we subjected an estimated 7.3 μg of purified material to nanomolar-scale NMR spectroscopic analysis (see Figure 3 in the Supporting Information).[20] The TOCSY, COSY, and HMBC spectra revealed three sets of cadaverine signals and two sets of succinyl signals (see Figures 22–26 in the Supporting Information). Long-range proton–carbon correlations between a methylene group of each cadaverine moiety and succinyl carbonyl groups indicated that the cadaverine and succinyl moieties were connected by an amide bond. Taking the fragment formula deduced by FTICR MS into consideration, we assigned the hydroxy groups as substituents on cadaverine nitrogen atoms and part of hydroxamate groups (see Figure 28 in the Supporting Information). Elucidation of the remaining NMR signals revealed an *anteiso*-branched alkyl chain, and the chain length was confirmed on the basis of fragmentation and the molecular formula (see Table 3 in the Supporting Information). Thus, promicroferrioxamine was determined to be a hydroxamate siderophore (Figure 2e). On the basis of this structure, the calculated mass (743.5646 Da, $[M+H]^+$) was within 0.0032 Da of that indicated by high-resolution mass spectrometry.

In summary, IMS of this marine environmental sample enabled the direct observation of numerous molecular signals. Two such molecules involved in metabolic exchange, previously uncharacterized, were further investigated and found to have different functions. First, we identified a peptide that prevents neighboring organisms from migrating into the territory of its producer: a functional phenotype not observed in liquid cultures. The second compound, a metabolite, is produced when there is competition for resources, such as iron. Our results suggest that such competition for iron may also exist under growth conditions with sufficient iron. In this study, we observed that promicroferrioxamine, a hydroxamate siderophore, is produced by *Promicromonosporaceae* strain SIO-11 in response to the presence of *B. subtilis* SIO-1. This competition also exists in liquid media, where we observed the production of promicroferrioxamine in response to the addition of SIO-1 (see Figure 21 in the Supporting Information). These two examples of molecules involved in metabolic exchange were found on the back of a barnacle and underscore the existence of many different chemical entities within environmental microbial interactions. Herein we have shown that IMS enables the visualization of such interactions in a microbial assemblage and that the signals observed are independent of the function and structural classification of the compounds detected.

Received: February 18, 2011
Revised: April 5, 2011
Published online: May 5, 2011

Keywords: bacteria · imaging mass spectrometry · metabolic exchange · NMR spectroscopy · siderophores

[1] B. L. Bassler, R. Losick, *Cell* **2006**, *125*, 237–246.
[2] P. D. Straight, R. Kolter, *Annu. Rev. Microbiol.* **2009**, *63*, 99–118.
[3] R. Dudler, L. Eberl, *Curr. Opin. Biotechnol.* **2006**, *17*, 268–273.
[4] K. Scherlach, C. Hertweck, *Org. Biomol. Chem.* **2009**, *7*, 1753–1760.
[5] E. A. Shank, R. Kolter, *Curr. Opin. Microbiol.* **2009**, *12*, 205–214.
[6] A. R. Pacheco, V. Sperandio, *Curr. Opin. Microbiol.* **2009**, *12*, 192–198.
[7] V. Schroeckh, K. Scherlach, H. W. Nützmann, E. Shelest, W. Schmidt-Heck, J. Schuemann, K. Martin, C. Hertweck, A. A. Brakhage, *Proc. Natl. Acad. Sci. USA* **2009**, *106*, 14558–14563.
[8] W.-T. Liu, Y.-L. Yang, Y. Xu, A. Lamsa, N. M. Haste, J. Y. Yang, J. Ng, D. Gonzalez, C. D. Ellermeier, P. D. Straight, P. A. Pevzner, J. Pogliano, V. Nizet, K. Pogliano, P. C. Dorrestein, *Proc. Natl. Acad. Sci. USA* **2010**, *107*, 16286–16290.
[9] C. D. Ellermeier, E. C. Hobbs, J. E. Gonzalez-Pastor, R. Losick, *Cell* **2006**, *124*, 549–559.
[10] J. E. González-Pastor, E. C. Hobbs, R. Losick, *Science* **2003**, *301*, 510–513.
[11] K. Yamanaka, H. Oikawa, H. O. Ogawa, K. Hosono, F. Shinmachi, H. Takano, S. Sakuda, T. Beppu, K. Ueda, *Microbiology* **2005**, *151*, 2899–2905.
[12] A. D'Onofrio, J. M. Crawford, E. J. Stewart, K. Witt, E. Gavrish, S. Epstein, J. Clardy, K. Lewis, *Chem. Biol.* **2010**, *17*, 254–264.
[13] D. S. Cornett, M. L. Reyzer, P. Chaurand, R. M. Caprioli, *Nat. Methods* **2007**, *4*, 828–833.
[14] K. Chughtai, R. M. Heeren, *Chem. Rev.* **2010**, *110*, 3237–3277.
[15] Y. L. Yang, Y. Xu, P. Straight, P. C. Dorrestein, *Nat. Chem. Biol.* **2009**, *5*, 885–887.
[16] A. Svatos, *Trends Biotechnol.* **2010**, *28*, 425–434.
[17] N. Bandeira, K. R. Clauser, P. A. Pevzner, *Mol. Cell. Proteomics* **2007**, *6*, 1123–1134.
[18] N. Bandeira, J. V. Olsen, J. V. Mann, M. Mann, P. A. Pevzner, *Bioinformatics* **2008**, *24*, 416–423.
[19] J. M. Vraspir, A. Butler, *Annu. Rev. Mar. Sci.* **2009**, *1*, 43–63.
[20] D. S. Dalisay, T. F. Molinski, *J. Nat. Prod.* **2009**, *72*, 739–744.

